

Relative X-Ray Backlighter Intensity Comparison of Ti and Ti/Sc Combination Foils Driven in Double- Sided and Single-Sided Laser Configuration

A. B. Bullock, O. L. Landen, D. K. Bradley

This article was submitted to *The Thirteenth Topical Conference on High-Temperature Plasma Diagnostics*, Tucson, Arizona, June 18-22, 2000

U.S. Department of Energy

Lawrence
Livermore
National
Laboratory

June 5, 2000

DISCLAIMER

This document was prepared as an account of work sponsored by an agency of the United States Government. Neither the United States Government nor the University of California nor any of their employees, makes any warranty, express or implied, or assumes any legal liability or responsibility for the accuracy, completeness, or usefulness of any information, apparatus, product, or process disclosed, or represents that its use would not infringe privately owned rights. Reference herein to any specific commercial product, process, or service by trade name, trademark, manufacturer, or otherwise, does not necessarily constitute or imply its endorsement, recommendation, or favoring by the United States Government or the University of California. The views and opinions of authors expressed herein do not necessarily state or reflect those of the United States Government or the University of California, and shall not be used for advertising or product endorsement purposes.

This is a preprint of a paper intended for publication in a journal or proceedings. Since changes may be made before publication, this preprint is made available with the understanding that it will not be cited or reproduced without the permission of the author.

This report has been reproduced
directly from the best available copy.

Available to DOE and DOE contractors from the
Office of Scientific and Technical Information
P.O. Box 62, Oak Ridge, TN 37831
Prices available from (423) 576-8401
<http://apollo.osti.gov/bridge/>

Available to the public from the
National Technical Information Service
U.S. Department of Commerce
5285 Port Royal Rd.,
Springfield, VA 22161
<http://www.ntis.gov/>

OR

Lawrence Livermore National Laboratory
Technical Information Department's Digital Library
<http://www.llnl.gov/tid/Library.html>

**Relative X-ray Backlighter Intensity Comparison of Ti and Ti/Sc Combination Foils
Driven in Double-Sided and Single-Sided Laser Configuration**

A. B. Bullock, O.L.Landen, and D.K. Bradley, *Lawrence Livermore National
Laboratory, Livermore CA.*

Abstract

Use of multiple backlighter foils and/or double-sided laser interaction geometry with backlit imaging can result in improved backlighter efficiency. An experimental comparison of backlighter intensity for Ti foils and Ti/Sc combination foils in both the one-sided and double-sided laser-interaction configuration is presented. Spectrally-integrated framing camera images show intensity contributions of front and rear backlighter surfaces for both foil types. Analysis of time-resolved x-ray spectra collected from foil targets show the relative contribution of Ti and Sc 2-1 He-like resonance lines to the total backlighter intensity.

Introduction

X-ray backlighting with laser-driven backlighter foils is an important diagnostic for laser-based high energy density experiments such as those using the Nova¹, Omega², and NIF³ high power laser facilities. Experiments studying implosions⁴ and planar Rayleigh-Taylor instabilities^{5,6} make use of area backlighters in the multi-kilovolt x-ray range. Experiments have examined the dynamics of laser-generated plasma in order to understand and maximize x-ray backlighter efficiency⁷ as a function of laser wavelength and pulsewidth. New techniques such as pinhole-assisted point projection backlighting⁸ will also benefit from improvements in area backlighter efficiency.

One method of increasing backlighter efficiency is to use a double-sided backlighter foil. A thin backlighter foil is illuminated on both sides by a high-energy laser pulse ($I=10^{14-15}$ W/cm²), and the x-ray emitted from laser-generated plasmas on both sides can contribute to the total backlighter emissivity. There are many advantages to this technique. A double-sided backlighter foil can potentially produce twice the x-ray flux of a single-sided backlighter at the same laser intensity level. This is very useful since beyond a certain laser intensity level, laser plasmas produce excessive amounts of high-energy x-rays which can reduce image contrast. Also, combining the emission of two plasma in the line of sight reduces the effect of spatial non-uniformities in the plasma.

Furthermore, double-sided backlighter foils allow laser beams from both in front and at the rear of the foil to interact with the backlighter, which is an advantage in laser facilities such as OMEGA and NIF. In question, however, is the amount of x-ray intensity which is lost due to backlighter foil reabsorption of the emitted x-rays. X-rays generated at the rear surface may be reabsorbed by the foil as the x-rays propagate through the foil and out the front foil surface³. One method of avoiding resonant reabsorption is to combine two different materials to form a composite foil 'sandwich'. By setting the lower Z foil at the rear, the line emission from the lower Z foil will propagate through the higher Z foil with minimal reabsorption since its emission is below the absorption edges of the higher Z foil.

In this paper, we study the emissivity of Ti and Sc/Ti double sided backlighter foils. The spectrally integrated emissivity from these foils as viewed from the front of the backlighter is compared to that from a single-sided Ti backlighter. Similarly, the summed emissivity of the Sc He_α and Ti He_α spectral lines for double-sided Ti and Sc/Ti backlighters measured in the front of the foil is compared to that of a single-sided Ti backlighter.

Experimental Description

The x-ray yield of Ti and Sc/Ti backlighter foils was studied with the method described below (see Figure 1). The 2 mm square backlighter foils consist of either a 12.7 μm Ti foil (see figure 1 (A)) or a 'sandwich' foil composed of a 7 μm Sc foil and a 7 μm Ti foil glued together with epoxy (see figure 1 (B)). The 'sandwich' Sc/Ti foil is oriented with the Sc at the rear and Ti at the front of the foil sandwich. Since the cold transmission of the Sc foil is very low for the Ti He_α spectral line (see figure 2), the Ti emission seen from the rear of the backlighter is minimal. However, the cold Ti foil transmission is reasonably high for the Sc He_α spectral line, and a large fraction of the Sc emission can propagate through the Ti foil without absorption. We would then expect the x-ray emission yield to be far higher at the front surface than at the rear, and therefore the x-ray yield measured at the front of the foil is the experimentally important value. Laser pulses from the OMEGA laser ($\lambda=351\text{ nm}$) illuminate the target with two laser spots at the front and one spot on the rear. The laser spot size is 250 μm , the laser pulse is a 3 ns square pulse ($\Delta I \approx 0.15 \langle I \rangle$), and the laser illuminates each spot with $750 \pm 12\text{ J}$. This produces an average laser intensity at each spot of approximately $5 \times 10^{14}\text{ W/cm}^2$. The upper laser spot on the front overlaps with the spot on the rear surface. The target is observed from the front by an x-ray framing camera placed at an angle of 40° from the foil normal. The framing camera has four microstrips, with 70 ps between images on a given strip and 750 ps delay between microstrips. This framing camera is sensitive to a wide range of x-ray

energies ($2 \text{ keV} < E < 10 \text{ keV}$), and the framing camera sensitivity is a weak function of x-ray energy in the range of 4 keV to 7 keV⁹. The pinhole array (20 μm pinhole diameter) in front of the framing camera images the foil plasma on the framing camera MCP with a x4 magnification.

Similar targets were used to measure the time-resolved x-ray spectra of the foils. In this case, laser pulses from the OMEGA laser illuminate the target with one spot in the front and one spot in the rear (see figure 1 (C)). The laser pulse shape, energy, spot size, and intensity are equal to that for the targets mentioned above. An x-ray streaked crystal spectrometer is placed in front of the foil at an angle of 40 degrees from the target normal to monitor the foil spectra. This spectrometer uses an RAP crystal and has a spectral coverage of 3.7-5.6 keV.

Experimental Results

Figure 3 shows framing camera images of the laser-generated plasmas for 2 types of foil at $t=1.0 \text{ ns}$. Here, the upper imaged spot is generated by x-rays emitted from plasmas from both sides of the foil. The lower spot is generated by a plasma facing the framing camera. In Figure 3 (A), the backlighter is a pure Ti foil and the top spot is generated by x-rays from a Ti plasma on both foil surfaces ('double-sided' laser-interaction configuration). The lower spot shown in this image is produced by the Ti laser

plasma on the surface facing the camera and is equivalent to a single-sided backlighter. Since there is a direct line-of-sight between this plasma and the framing camera, all Ti spectrum lines can reach the framing camera MCP without absorption. Similarly, the Ti plasma on the surface facing the camera for the upper laser spot can also reach the MCP without reabsorption. X-rays from the Ti plasma formed on the rear foil surface must propagate through the Ti foil prior to arrival at the framing camera. The colder regions of this foil will act as a filter, preferentially absorbing the higher energy Ti lines. Since the x-rays from this plasma propagate to the framing camera at a 40 degree angle relative to the backlighter normal, the x-rays propagate through 16.6 μm of Ti. Figure 4 (A) shows an x-ray spectra produced by a Ti plasma illuminated by a laser pulse of intensity $5 \times 10^{14} \text{ W/cm}^2$. Shown in Figure 4 (B) is the calculated x-ray spectra after filtering by a 16.6 μm Ti foil, in which the filtering effect of the backlighter foil can clearly be seen. This indicates that the x-ray fluence produced by the spots on the other side of the framing camera will be composed primarily of the Ti He_{α} and associated satellites ($\approx 4.7 \text{ keV}$). In figure 3 (B), the backlighter is a Sc/Ti foil. In this case, the laser generates a Ti plasma facing the camera at both the top and bottom of the foil, and the laser generates a Sc plasma on the rear surface of the foil. X-rays generated by the Sc plasma which reach the camera propagate through the Sc/Ti foil, and this sandwich foil also acts like a filter. In this case, the x-ray fluence which arrives at the framing camera will be composed

primarily of Sc He_α (4.29-4.32 keV) which is the only relevant Sc transition below the cold Sc K edge at 4.5 keV. Figure 5 shows the ratio of total spatially-integrated x-ray energy between the top and bottom spots shown in Figure 2 as a function of time for both Ti and Sc/Ti foils. Since the bottom spot is produced by single-sided Ti backlighter, the ratio shown in figure 5 is the ratio of double-sided x-ray yield for Ti and Sc/Ti backlighters to the yield for a single-sided Ti backlighter. The energy ratio measured for the double-sided Ti foil is roughly similar to that measured for the Sc/Ti foil. This indicates that, within the error of the measurement, the emissivity below the respective cold K edges for the Ti and Sc/Ti foils is the same. This plot also shows that the time-averaged broadband emissivity of the double-sided Ti backlighter is approximately 60% larger than that of a single-sided Ti backlighter in early time ($t < 1$ ns), while the time-averaged emissivity of the Sc/Ti backlighter is approximately 20 % greater than that of a single-sided Ti backlighter in early time ($t < 1$ ns).

Figure 6 shows the emitted spectra recorded by the streaked spectrometer of a double-sided Ti x-ray spot and a double-sided Sc/Ti x-ray spot at $t = 860$ ps. This spectra is recorded from the laser interaction geometry shown in figure 1 (C), and there is one overlapping laser spot on front and rear of the sandwich foil. The Sc He_α and the Ti He_α is clearly shown. Recorded spectra allows us to measure the relative He_α line emission of the double-sided Ti and Sc/Ti foils compared to that of a single-sided Ti backlighter.

Since the spectra shown for the Sc/Ti double-sided backlighter in the energy range 4.6 keV to 4.9 keV is produced entirely by the Ti He $_{\alpha}$ emission from the Ti plasmas facing the spectrometer, we integrate the Sc/Ti spectral intensity in the range of 4.6 keV to 4.9 keV to get the integrated Ti He $_{\alpha}$ intensity of the single-sided Ti backlighter. Integrating the double-sided Ti spectra over this spectral gives the integrated Ti He $_{\alpha}$ intensity of the double-sided Ti backlighter. Figure 7 shows the ratio of Ti He $_{\alpha}$ intensity for double-sided and single-sided backlighter spots. We integrated the Sc/Ti spectra in the range of 4.2 keV to 4.9 keV to sum the intensity of both the Sc He $_{\alpha}$ and the Ti He $_{\alpha}$ lines. The ratio of this integrated intensity to the integrated Ti He $_{\alpha}$ intensity of the single-sided Ti backlighter is also shown in Figure 7. The figure shows that, within the error of the measurement, the time-averaged Ti double-sided backlighter emissivity in this range of x-rays energies is approximately 80% greater than that of a single-sided backlighter in early time ($t < 1\text{ns}$). The Sc/Ti double-sided backlighter emissivity in this range of x-rays energies is approximately 40% greater than that of a single-sided Ti backlighter in early time ($t < 1\text{ns}$).

Conclusions

The relative x-ray yields of double-sided Ti and Sc/Ti backlighter foils were compared to a single-sided backlighter foil. The time-averaged broadband (4.0-7.0 keV)

double-sided Ti backlighter emissivity is 60% greater than that of the single-sided Ti backlighter in early time ($t < 1\text{ ns}$), and the time-averaged narrow band (4.2–4.9 keV) double-sided Ti backlighter emissivity is 80% greater than that of the single-sided Ti backlighter in early time ($t < 1\text{ ns}$). The time-averaged broadband (4.0–7.0 keV) double-sided Sc/Ti backlighter emissivity is 20% greater than that of the single-sided Ti backlighter in early time ($t < 1\text{ ns}$), and the time-averaged narrow band (4.2–4.9 keV) double-sided Sc/Ti backlighter emissivity is 40% greater than that of the single-sided Ti backlighter in early time ($t < 1\text{ ns}$).

This work was performed under the auspices of the U.S. Department of Energy by the University of California, Lawrence Livermore National Laboratory under Contract No. W-7405-Eng-48.

¹ KilKenny, J.D., Phys. Fluids B **2**, 1400 (1990).

² Soures, J.M., et.al., Phys. Plasmas, **3**, 2108 (1996).

³ Landen, O.L., HTPD 2000 reference

⁴ Turner, R.E., et.al., Phys. Plasmas **7**, 333 (2000).

⁵ Glendinning, S.G., et.al., Phys. Rev. Lett. **69**, 1201 (1992).

⁶ Remington, B.A., et. al., Phys. Rev. Lett., **73**, 2589 (1993).

⁷ Mathews, D.E., et.al., J. Appl. Phys., **54**, 4260 (1983).

⁸ Bullock, A.B., Landen, O.L., Bradley, D.K. submitted the HTDC 2000 conference.

⁹ Yamaguchi, N., Cho, T., Kondoh, T., Hirata, M., Miyoshi, S., Aoki, S., Maezawa, H., and Nomura, M., Rev. Sci. Instrum. **60**, 368 (1989).

Table of Figures

Figure 1. Diagram of laser target. The backlighter foil consists of either a $12.7\text{ }\mu\text{m}$ Ti foil or a combination foil composed of $7\text{ }\mu\text{m}$ of Sc and $7\text{ }\mu\text{m}$ of Ti. In (A) and (B), the target is observed by a x-ray framing camera. In (B), this framing camera is placed on the same side as the Ti foil. In (C), the streak camera is placed on the same side as the Sc foil.

Figure 2. Plot of cold Ti and Sc x-ray transmission for x-rays propagating into the x-ray framing camera. Here the absorption is calculated using a pathlength of $9.1\text{ }\mu\text{m}$, since the framing camera is placed 40 degrees from the surface normal of each $7\text{ }\mu\text{m}$ foil.

Figure 3. Images of laser-generated plasma on foil surface. In (A), the backlighter is Ti, and in (B), the backlighter is Sc/Ti. The upper spot is produced by x-rays generated by laser plasma on both foil surfaces. The bottom spot is generated by laser plasma on the front Ti surface (a 'single-sided' backlighter). The framing camera is placed to view the Ti front foil surface.

Figure 4. Plot of Ti backlighter spectra. Spectra (A) shows the emission from a Ti plasma with an unobstructed line-of-sight to the spectrometer. Spectra (B) show the calculated emission spectrum after filtering by a cold $16.6\text{ }\mu\text{m}$ Ti foil. The spectrometer is placed to view the Ti front foil surface.

Figure 5. Plot of the ratio of x-ray yield for double-sided Ti and Sc/Ti backlighters to the yield for a single-spot Ti backlighter ('single-sided' Ti backlighter).

Figure 6. Plot of the He-alpha x-ray spectra emitted from a double-sided Ti foil and a Sc/Ti foil at a time $t = 860\text{ps}$. Note that this spectra is produced by a single spot on the front and rear foil surfaces.

Figure 7. Plot of the ratio of x-ray emissivity of double-sided Ti and Sc/Ti backlighter to that of a single-sided Ti backlighter spots for the x-ray range 4.2 keV to 4.9 keV. As shown in figure 5, this energy range included only the Ti and Sc He_α spectral lines.

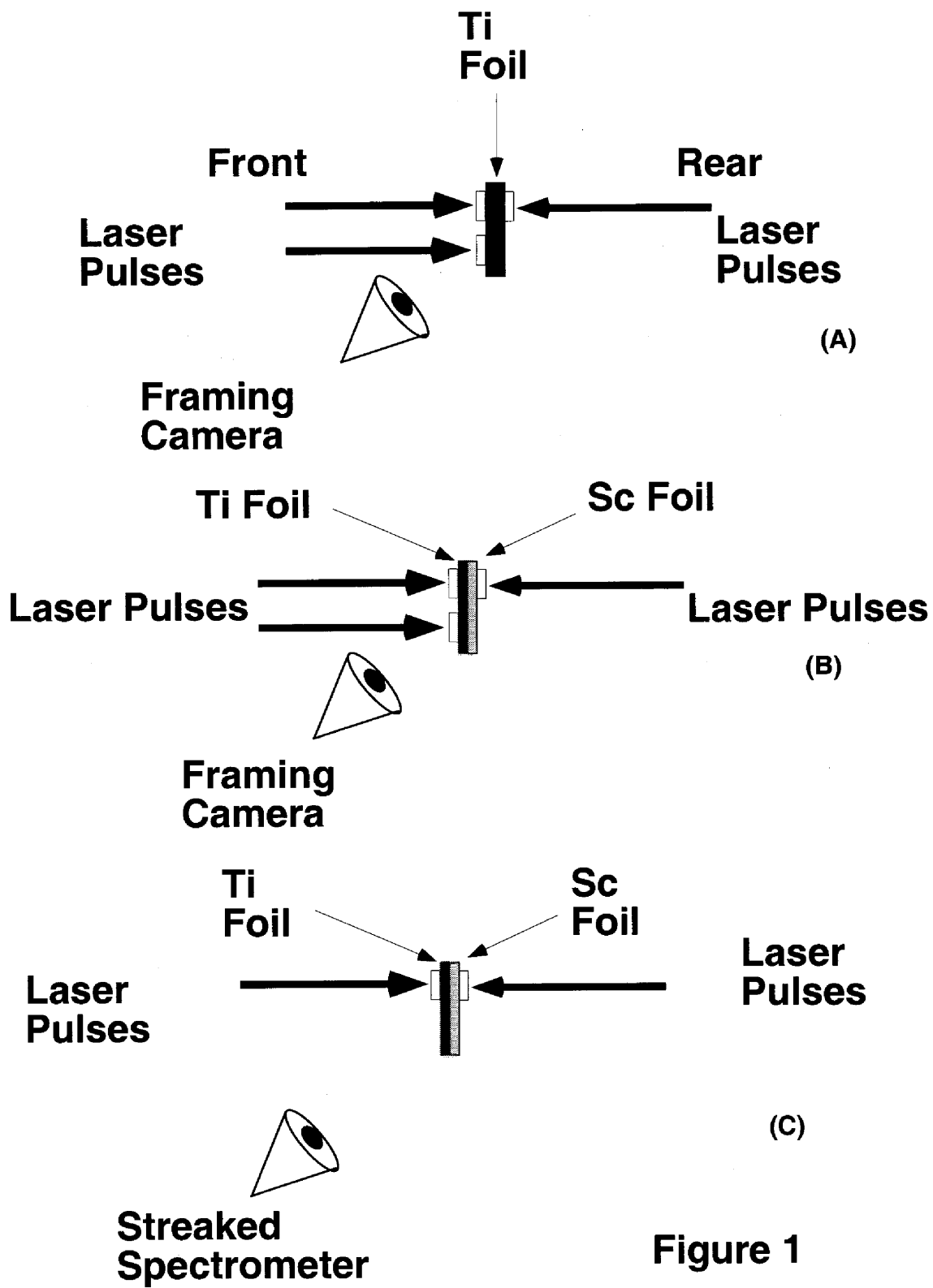


Figure 1

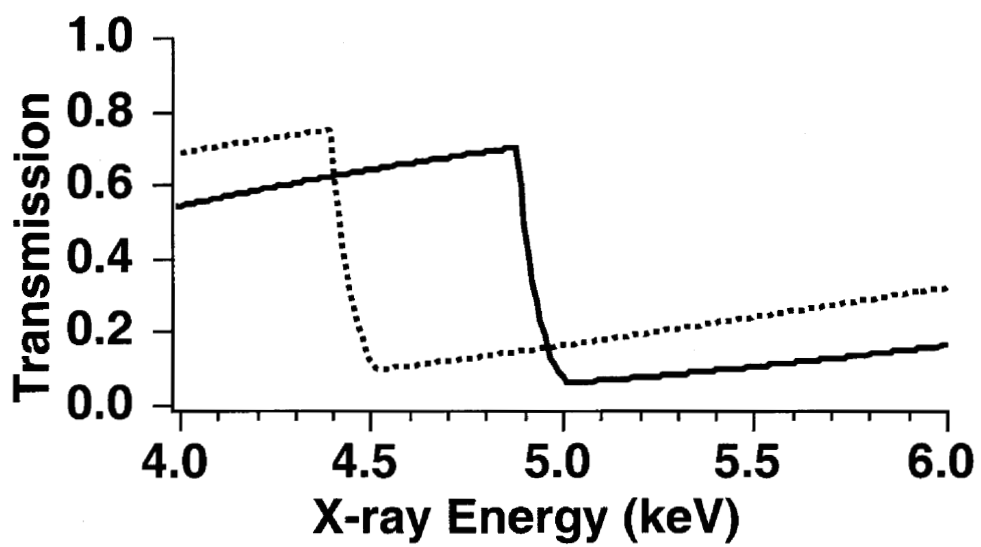


Figure 2

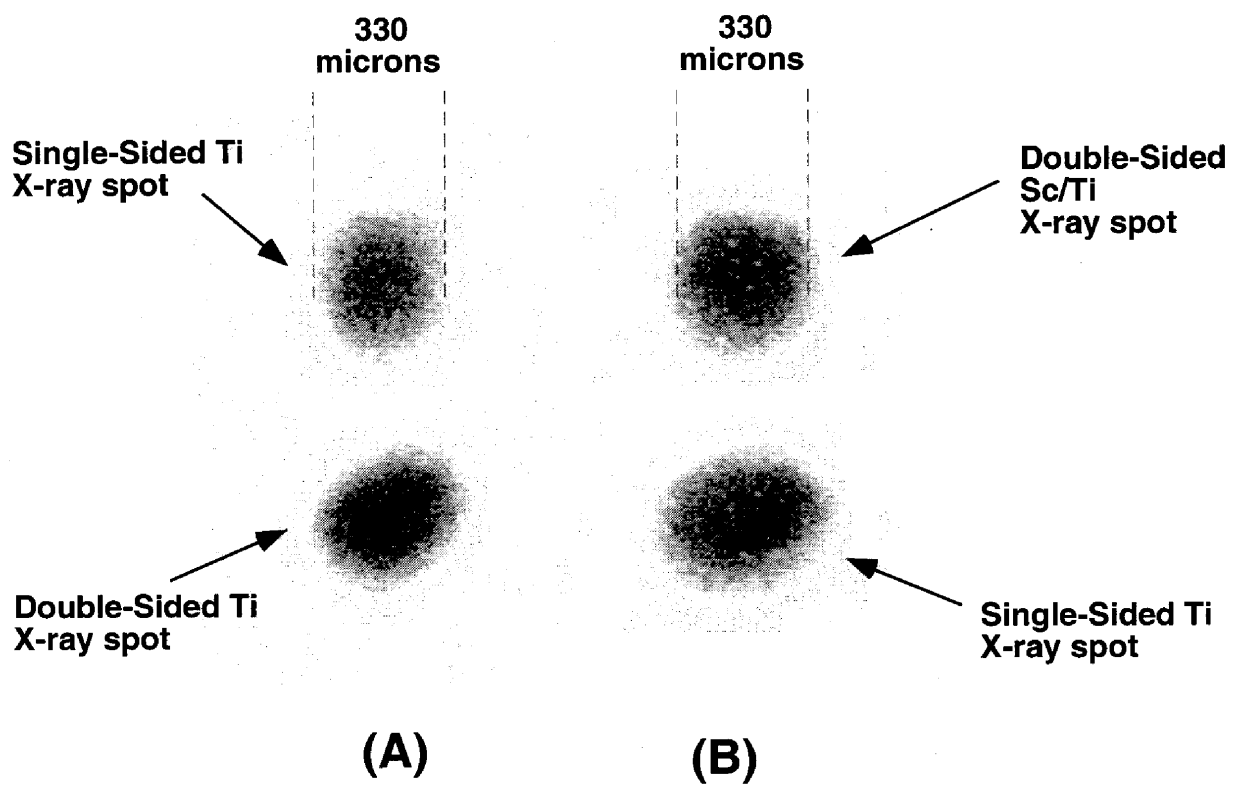


Figure 3

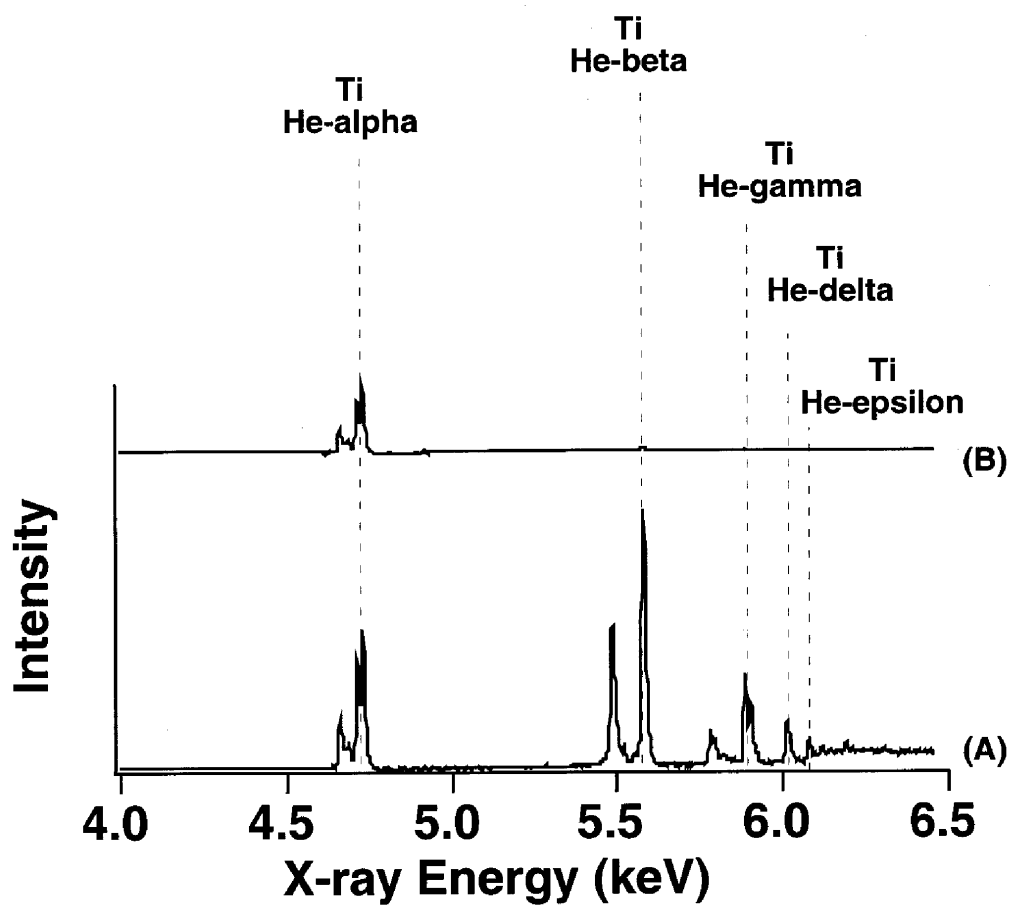


Figure 4

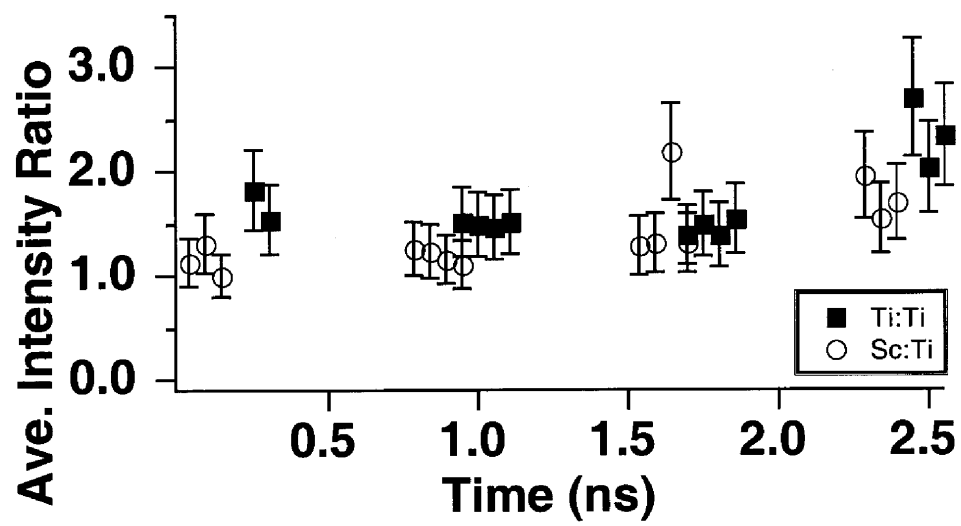


Figure 5

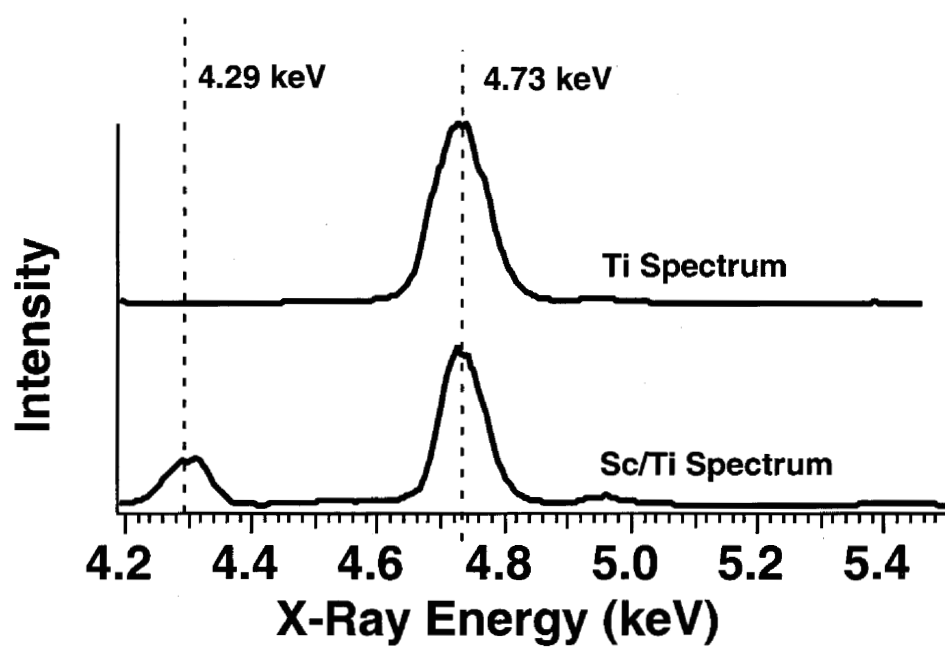


Figure 6

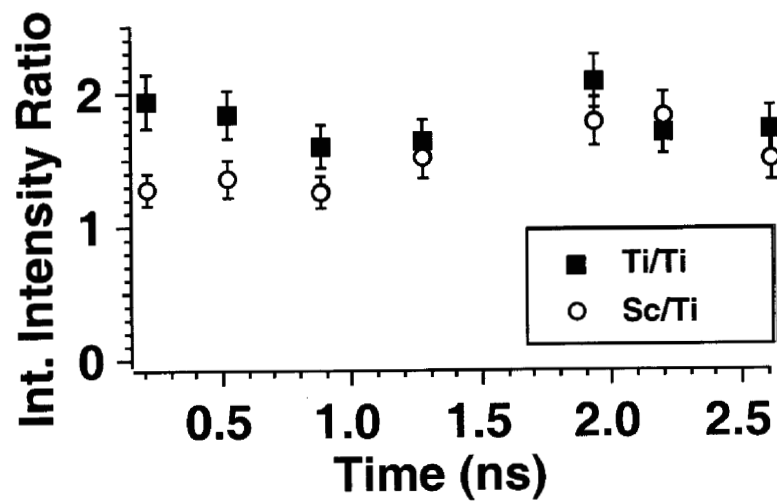


Figure 7